Contents lists available at SciOpen

Food Science and Human Wellness

journal homepage: https://www.sciopen.com/journal/2097-0765

China Food Publishing Co.

Heterologous expression, purification and characterization of *Lactobacillus acidophilus* CICC6074-derived slpX protein and the molecular mechanism of its anti-inflammatory effect on LPS-induced RAW264.7 cells

Yingying Cao[a,b], Xiankang Fan[a,b], Zihang Shi[a,b], Mingzhen Liu[a,b], Jue Xu[a,b], Tao Zhang[a,b], Xiaoqun Zeng[a,b], Zhen Wu[a,b], Daodong Pan[a,b,*]

[a] *State Key Laboratory for Managing Biotic and Chemical Threats to the Quality and Safety of Agro-products, Ningbo University, Ningbo 315211, China*
[b] *Key Laboratory of Animal Protein Food Deep Processing Technology of Zhejiang Province; Food & Pharmaceutical Sciences College of Ningbo University, Ningbo 315211, China*

ARTICLE INFO

Article history:
Received 1 November 2023
Received in revised form 30 November 2023
Accepted 21 December 2023

Keywords:
Lactic acid bacteria
S-layer protein
Inflammation
Liquid chromatography-tandem mass spectrometry
Enzyme-linked immunosorbnent assay
Molecular docking

ABSTRACT

The role of S-layer proteins (SLP), which form the outermost layer of cell walls in lactic acid bacteria (LAB), plays a crucial role in regulating immune-stimulating activity, thereby closely influencing LAB's ability to boost host immunity. In this study, the heterologous expression, purification, and characterization of *Lactobacillus acidophilus* CICC6074-derived slpX protein and the molecular mechanism of its anti-inflammatory effect on LPS-induced RAW264.7 cells were investigated. Initially, the PCR results were shown to successfully clone the slpX DNA sequence by homologous recombination to obtain the pet-32a-slpX recombinant plasmid. SDS-PAGE results revealed that slpX protein with a molecular weight of 54 kDa was successfully obtained under 0.7 mmol/L IPTG-induced conditions, which was further demonstrated by Western blot (WB) and LC-MS/MS. ELISA, WB and molecular docking results indicated that slpX protein can inhibit LPS-induced cellular inflammatory responses by linking to TLR4 and MD2 *via* hydrogen bonding and increasing the levels of anti-inflammatory factor IL-10 and decreasing the levels of inflammatory factors (TNF-α, IL-6, NO) and ROS *via* MAPK and NF-κB signaling pathways. The study is essential for the preparation of pure slpX protein and revealing its anti-inflammatory molecular mechanism.

1. Introduction

Lactic acid bacteria (LAB) are Gram-positive, anaerobic or microaerophilic bacteria[1]. They are usually found in dairy products, meat and fermented products[2]. And some LAB are often considered as beneficial microorganisms due to their mucosal tolerance, ability to stimulate the immune response and resistance to disease[3]. These microorganisms encounter a harsh inorganic acidic environment when they enter the human gastrointestinal tract, Zhang et al.[4] found that Mn^{2+} pre-stress increases the acid tolerance of *Lactobacillus acidophilus* CICC6074 through the secretion of S-layer proteins. S-layer proteins also help *Lactobacillus* to colonise the gut, mediate bacterial adhesion to host cells and modulate the intestinal immune response[5-6]. In addition, S-layer proteins are crystalline arrays of protein subunits that form a single molecule and are found in both Gram-positive and Gram-negative bacteria, as well as archaea[7]. These proteins attach to the cell surface through non-covalent interactions and play a crucial role in maintaining cell morphology, inhibiting pathogenic bacterial adhesion, and modulating host immunity against viruses[8-9]. The S-layer proteins found in

* Corresponding author at: State Key Laboratory for Managing Biotic and Chemical Threats to the Quality and Safety of Agro-products, Ningbo University, Ningbo 315211, China
E-mail address: daodongpan@163.com (D.D. Pan)
Peer review under responsibility of Beijing Academy of Food Sciences.

Publishing services by Tsinghua University Press

http://doi.org/10.26599/FSHW.2024.9250230

L. acidophilus have been shown to reduce bacterial viability and may act as novel enzymatic antimicrobial agents[10], making them a promising avenue for future research in the field of antimicrobial therapy. Using the HT-29 cell model, Xue et al.[11] observed that removal of S-layer proteins from *L. acidophilus* decreased the ability of *L. acidophilus* to inhibit intestinal pathogens, suggesting that the S-layer proteins are involved in probiotic adherence, implying that S-layer proteins have an excellent adherence capacity. This property helps *Lactobacillus* to maintain immune homeostasis while having higher inhibitory capacity against[12]. Suzuki et al.[9] constructed truncated and chimeric S-layer proteins in *Escherichia coli*, which acted on human monocytic leukaemia cells (THP-1), and found that the intact conformation of the N-terminal region of SLP contributes to the high immunogenicity and enhances the anti-inflammatory capacity of the organism.

Inflammation is a highly self-regulated process, with transient inflammatory responses serving to induce stress protection and investigate and clear invading pathogens[13]. However, excessive inflammatory responses can lead to tissue damage and autoimmune diseases[14], such as arthritis, inflammatory bowel disease, atherosclerosis and cancer[15]. When the body is invaded by pathogens, it causes monocytes in the blood to differentiate into macrophages. Macrophages play a key role in the process of innate and adaptive immunity[16]. Activated macrophages secrete pro-inflammatory factors such as tumour necrosis factor-α (TNF-α), IL-6 and the pro-inflammatory mediator nitric oxide (NO) to modulate host defence mechanisms[17]. For example, Gao et al.[10] found that incubation with S-layer proteins inhibited H9N2 virus invasion of mouse dendritic cells (DCS) to reduce the mRNA expression of haemagglutinin (HA) and neuraminidase (NA). From *L. kefiri* Slp from CIDCA8348 was able to enhance ova-specific immune response by recognising the glycan fraction through Mincle to trigger maturation of antigen-presenting cells[18]. S-layer proteins, including slpA, slpB and slpX, have been identified to date, but studies on S-layer proteins remain at the whole protein level. Currently, there are no studies on anti-inflammatory immunity of slpX, in addition the site of action of slpX on inflammation and its regulatory mechanisms are not clear.

In this study, the gene fragment encoding slpX protein in *L. acidophilus* CICC6074 was obtained by PCR, which was ligated to the pet-32a plasmid to constitute a recombinant expression plasmid, and the recombinant plasmid was introduced into *E. coli* BL21 (DE3) to construct a prokaryotic expression strain. The slpX protein was obtained after induction purification. The correctness of the protein was verified by Western blot (WB) and liquid chromatography-tandem mass spectrometry LC-MS/MS). The anti-inflammatory effect of slpX protein was assessed by constructing RAW264.7 inflammatory cell model. Molecular docking was used to explain the anti-inflammatory mechanism of slpX protein. We hope that our study contributes to a deeper understanding of the probiotic role of *Lactobacillus* S-layer proteins.

2. Materials and methods

2.1 Materials

L. acidophilus CICC6074 was preserved at the China General Microbiology Culture Collection Centre (CGMCC, Beijing, China). The RAW264.7 cell was obtained from Wuhan Pronosai Life Sciences Co., Ltd. (Wuhan, China). Cell counting kit-8 (CCK-8), 4-amino-5-methylamino-2′,7′-difluorofluorescein (DAF-FMDA), total nitrogen assay kit, 2,7-dichlorodihydrofluorescein diacetate (DCFH-DA) and LPS were all purchased from Beyotime (Shanghai, China), mouse TNF-α, IL-6 and IL-10 enzyme-linked immunosorbent assay (ELISA) kits were purchased from Multi Sciences (Hangzhou, China). Antibodies used in the experiments were purchased from ABclonal Technology and Cell Signaling Technology (Wuhan, China). The chemicals used in this experiment were all analytical grade.

2.2 Construction of pet-32a-slpX expression vector

DNA samples were extracted from *L. acidophilus* CICC6074 using the TIANamp Bacterial DNA Kit (Tiangen Biotechnology Co., Ltd., Beijing, China) according to the manufacturer's instructions. The primers used to construct the pet-32a-slpX recombinant plasmid were designed using CE design software with primer sequences F1 (5′-TTAATAGAAGTTTACAGCCTTG-3′) and R1 (5′-AGGAGATAACTATAAATGAAG-3′). The *slpX* gene fragment was amplified using PCR with the following PCR procedure: (95 °C pre-denaturation for 3 min, 95 °C annealing for 15 s, 55 °C annealing for 15 s, 72 °C for 2 min, 72 °C for 5 min, and 35 cycles). The PCR product was purified using an agarose gel DNA purification kit (Omega Bio-Tek, USA). The pet-32a plasmid was linearised by *NcoI* and *HindIII* restriction endonucleases. The *slpX* gene fragment was ligated to the linearised pet-32a vector using a one-step cloning kit and introduced into *E. coli* BL21 (DE3) receptor cells (Vazyme Biotech, Nanjing, China). It was spread on LB plate containing 100 μg/mL ampicillin and cultured at 37 °C for 18 h. Positive colonies were picked for PCR verification, and the successfully constructed recombinant strains were stored for spare use.

2.3 SlpX protein purification

The constructed *E. coli* BL21 pet-32a-slpX strain was inoculated into LB medium containing ampicillin (Amp, 100 μg/mL) and induced by adding 0.7 mmol/L IPTG. Induction was incubated at a low temperature of 25 °C for 16 h. Bacteria were collected, centrifuged and the supernatant discarded, then the bacteria were washed twice with sterile PBS (6 000 r/min, 10 min). The cell was sonicated using an ultrasonic cell crusher. After ultrasonic disruption (every 5 s for a total of 250 times), the supernatant was collected by centrifugation at 4 °C (12 000 r/min for 30 min) and filtered through 0.22 μm sterile filter membrane. The target protein was purified using Ni-NTA 6FF agarose purification resin (Sangon Biotech, Shanghai, China). Equilibration buffer (50 mmol/L sodium dihydrogen phosphate, 300 mmol/L NaCl, 10 mmol/L Tris-HCl, 10 mmol/L imidazole, pH 8.0), elution buffer (50 mmol/L sodium dihydrogen phosphate, 300 mmol/L NaCl, 10 mmol/L Tris-HCl, 10 mmol/L imidazole, pH 8.0). The collected proteins were dialyzed in cooled PBS buffer (4 °C) and the protein concentration was measured with a BCA kit (Takara, Beijing, China).

2.4 Validating 6× His tags

The slpX proteins were denatured by adding denaturing buffer and cooking at 100 °C for 10 min, and the proteins were linearly

separated using a protein gel with a gel concentration of 10%. The PVDF membrane was closed with 5% skimmed milk buffer for 1 h. The membrane was then incubated overnight at 4 °C with the corresponding primary antibody and then incubated with the secondary antibody for 1 h at room temperature. Finally, the protein bands were detected with an enhanced chemiluminescence kit (ECL) (Yoche, Shanghai, China).

2.5 Cell culture and viability assay

RAW264.7 macrophages were cultured in an incubator containing 5% carbon dioxide and a complete medium (1% penicillin-streptomycin and 10% fetal bovine serum). Cells were passaged when they reached 80%−90% fusion. 2×10^4 RAW264.7 cells were inoculated into 96-well plates and cultured overnight. The cells were divided into blank, control and slpX-treated groups, only PBS was added in the blank group, the cells grew normally in the control group, and the experimental group was treated with different concentrations of slpX (5, 10, 50, 100, and 200 μg/mL) for 24 h. After the cells were treated with different concentrations of slpX (5, 10, 50, 100, and 200 μg/mL), 20 μL of CCK-8 solution was added and cultured for 2 h in the incubator. Absorbance was measured at 540 nm using an enzyme marker (Tecan, Switzerland). The optimal stimulation time and concentration of LPS were determined using the same method. Cell morphology was observed under an inverted microscope after 6 h of pretreatment with slpX protein and 18 h of LPS stimulation of cells.

2.6 ELISA evaluation

ELISA was used to quantify TNF-α, IL-6 and IL-10 secretion levels in cell supernatants according to the manufacturer's instructions. Briefly, RAW264.7 macrophages (1×10^5 cells/mL) were cultured in 12-well plates, pretreated with slpX protein (5, 10, 50 and 100 μg/mL) for 6 h, and then LPS (1 μg/mL) was added for 18 h. The supernatant was collected and the cell suspension was discarded after centrifugation (14 000 r/min, 15 min) and then the levels of TNF-α, IL-6 and IL-10 were determined by enzyme-linked immunosorbent assay.

2.7 NO assay

RAW264.7 macrophages (1×10^5 cells/mL) were inoculated into 12-well plates and cultured for 16 h. The cells were then pretreated with slpX protein (5, 10, 50 and 100 μg/mL) for 6 h. The cells were then incubated in a 12-well plate and then pretreated for 6 h with slpX protein (5, 10, 50 and 100 μg/mL). The Griess method and ELISA (Beyotime, Shanghai, China) were used to evaluate the release of NO, respectively.

2.8 ROS fluorescence intensity

The formation of intracellular ROS was analysed using DCFH-DA to make qualitative observations of the fluorescence intensity of the cells, as described by Subhan et al.[19]. RAW264.7 macrophages (1×10^5 cells/mL) were inoculated into 12-well plates and cultured for 16 h. Cells were pretreated with slpX protein (5, 10, 50, and 100 μg/mL) for 6 h. Cells were then stimulated with LPS (1 μg/mL) for 18 h. The culture medium was discarded, 300 μL of DCFH-DA (10 μmol/L in serum-free medium) probe was added dropwise to each well, and the cells were incubated for 20 min at 37 °C and 5% CO_2 in a cell incubator protected from light. After removing the cells, sterile PBS was rinsed, and the ROS content in the cells was observed with an inverted fluorescence microscope, photographed and recorded.

2.9 Immunofluorescence staining

Activation of NF-κB nuclear translocation was detected using the NF-κB activation-nuclear translocation assay kit (Beyotime Biotechnology, Shanghai, China) with a slight modification of the method described by Athapaththu et al.[20]. The details were as follows: log phase RAW264.7 cells were inoculated overnight in glass-bottomed dishes at 1×10^5 cells/well. After the cells were coated and treated with the grouping described above, the cells were treated with slpX (5, 10, 50 and 100 μg/mL) for 2 h, followed by stimulation with LPS (1 μg/mL) for 1 h. Cells were fixed with fixation buffer for 15 min, and immunostaining blocking solution was added and blocked for 1 h at room temperature. NF-κB p65 mouse monoclonal antibody was added and incubated overnight at 4 °C. Cells were then incubated with cy3-coupled secondary antibody for 1 h at room temperature, protected from light, and stained with 4,6-diamino-2-styryl alcohol (DAPI) for 5 min.

2.10 WB analysis

Cells were inoculated at a density of (2×10^5 cells/well) into a 6-well plate and incubated overnight, cells were removed from the incubator and placed on ice, the culture fluid was aspirated and washed twice with ice-cold PBS, 200−300 μL of lysis buffer (RIPA buffer and protease inhibitor) was added to each well and incubated for 5 min on ice, with occasional shaking in between. Samples were collected and shaken on a shaker at 4 °C for 15 min to promote further cell lysis. The samples were centrifuged in a pre-cooled 4 °C centrifuge at 14 000 r/min for 15 min, and the supernatant obtained from centrifugation was transferred to the new tubes. Cell protein storage and denaturation treatment: add denaturation buffer and cook at 100 °C for 10 min, and finally store the protein product at −80 °C. The protein concentration after lysis was determined using BCA kit. The amount of protein samples was adjusted according to the protein concentration, and protein gels with a gel concentration of 10% were used for linear separation of proteins. WB steps are consistent with section 2.4. The grey scale was analysed using ImageJ software.

2.11 Molecular docking

Human TLR4/MD2 complex [protein data bank (PDB) ID: 3FX1] and mouse TLR4/MD2 complex (PDB ID: 3VQ2) and slpX protein (PDB ID: 7QFI) crystal structures were obtained from the PDB (https://www1.rcsb.org) and all non-amino acids were removed. Water molecules, hydrogenation, and charge were removed from the proteins using Discovery Studio (DS) software, and the processed proteins were visualised using pymol. Docking calculations of proteins were performed using ZDOCK.

2.12 Statistical analysis

All experiments were repeated three times. Statistical analysis of data was performed using SPSS 22.0 for analysis of variance (ANOVA) with a $P < 0.05$ level of difference of 0.05, and Origin 2019b was used for graphic production.

3. Results and discussion

3.1 Validation of pet32a-slpX recombinant plasmid and purified slpX protein

S-layer proteins are regular structures on the outer surface of bacteria that are widely distributed in archaea, Gram-negative and Gram-positive bacteria[21], and have a variety of pharmacological properties, including anti-phage, anti-inflammatory, anticancer, and inhibition of pathogenic bacteria[11,18,22]. Primers were designed to target the *slpX* gene sequence in the S-layer protein and the PCR products were validated on a 1% agarose gel. The target gene was well labelled and approximately the same size as the *slpX* gene (Fig. 1A). The *slpX* gene was expressed in the presence of the T7 promoter and the recombinant plasmid is shown in Fig. 1B. Under the induction condition of 0.7 mol/mL IPTG, after ultrasonic crushing and induced purification, a high-purity slpX band with molecular weight of about 54 kDa was finally obtained, which was the same as the theoretical value (Fig. 1C), and it was further confirmed that the protein obtained was slpX by LC-MS/MS(supplementary material). The single band obtained was further verified to be the slpX protein by the WB assay (Fig. 1D). Prokaryotic expression was performed using the *E. coli* system with low transformation costs compared to S-layer proteins extracted with LiCl[23]. Using prokaryotic expression to obtain proteins not only makes the proteins more precise, but also increases the yield of proteins, making experiments easier.

3.2 Cell cytotoxicity

The CCK-8 assay is highly sensitive and radioactive and was used to detect the toxic effects of slpX proteins on cells and to analyse their effects on cell viability[24]. As shown in Fig. 2A, the effects on cell viability were examined at 5 concentration gradients of 5, 10, 50, 100 and 200 μg/mL. However, when the concentration of slpX was 200 μg/mL, the cell viability showed a significant decline, and the survival rate decreased to 35.55%, which had a certain degree of damage to the cells. Therefore, the concentrations of slpX (5, 10, 50 and 100 μg/mL) were chosen for subsequent experiments. To determine the optimal concentration and stimulation time for the effect of LPS, cells were treated with different concentrations (0.2, 0.4, 0.6, 0.8 and 1.0 μg/mL) and times (6 and 18 h). When the stimulation time of LPS (1 μg/mL) was 18 h, the cell viability was drastically reduced and the viability was only 52.70% (Fig. 2B), which was a significant change compared to the control group. The optimal stimulation effect was achieved. Therefore, LPS (1 μg/mL) was chosen to stimulate RAW264.7 cells for 18 h as the optimal concentration and time of action of LPS. Fig. 2C shows that the number of cells treated with LPS was also reduced, and the number of cells was significantly higher in the third graph; the cell morphology gradually improved after 6 h of pretreatment with slpX protein compared with LPS alone. This provided the basis for the later validation of the anti-inflammatory function of slpX.

3.3 Alteration of LPS-induced RAW264.7 macrophage cytokines by slpX protein

Lipopolysaccharide (LPS) releases inflammatory factors by triggering macrophage and neutrophil release[25-27], such as IL-6, TNF-α[28]. In Fig. 3A, cells not stimulated with LPS secreted lower levels of TNF-α ((48.9 ± 2.2) pg/mL), however, after stimulation of the cells with LPS, the release of TNF-α increased dramatically ((1 149.5 ± 6.2) pg/mL), and when the cells were pre-incubated with 5−100 μg/mL of slpX protein the level of TNF-α decreased significantly, and when the cells were pre-incubated with levels of TNF-α were significantly decreased when cells were preincubated with 100 μg/mL of slpX protein. The secretion level of TNF-α in the cells decreased dramatically ((950.99 ± 12.90) pg/mL) when 100 μg/mL slpX protein was used and was significantly higher than the inhibitory ability of Slp protein on TNF-α as studied by Wang et al.[29]. It was further shown that the slpX protein in the S-layer proteins had superior anti-inflammatory properties and could inhibit the release of inflammatory factors in a concentration-dependent manner. Whereas, some researchers have suggested that the MAPK signalling

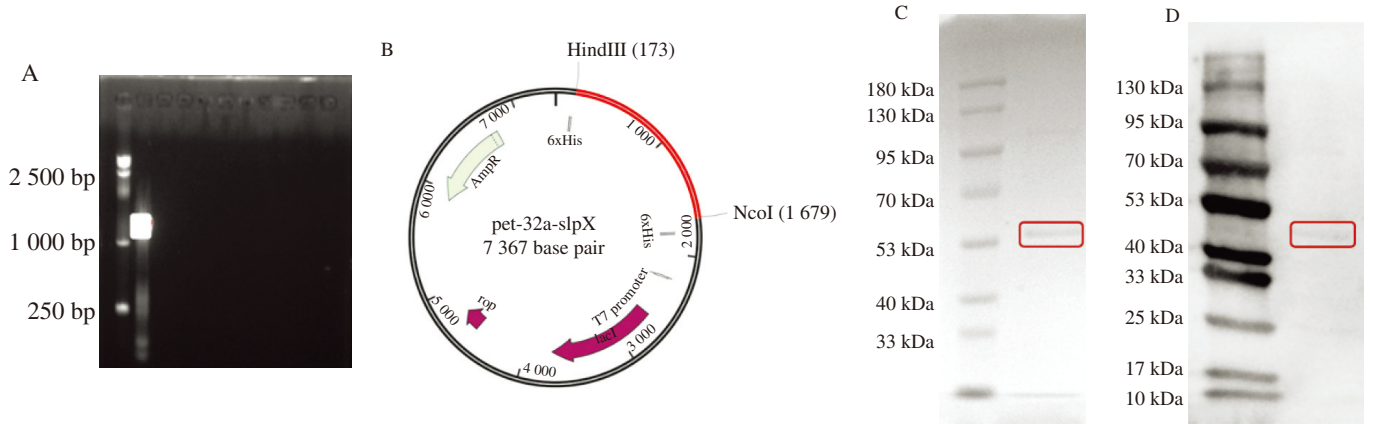

Fig. 1 Construction and purification of slpX protein vector. (A) PCR amplification product of slpX. (B) pet-32a-slpX protein recombinant plasmid. (C) SDS-PAGE identification of recombinant slpX protein. (D) slpX-His tag validation.

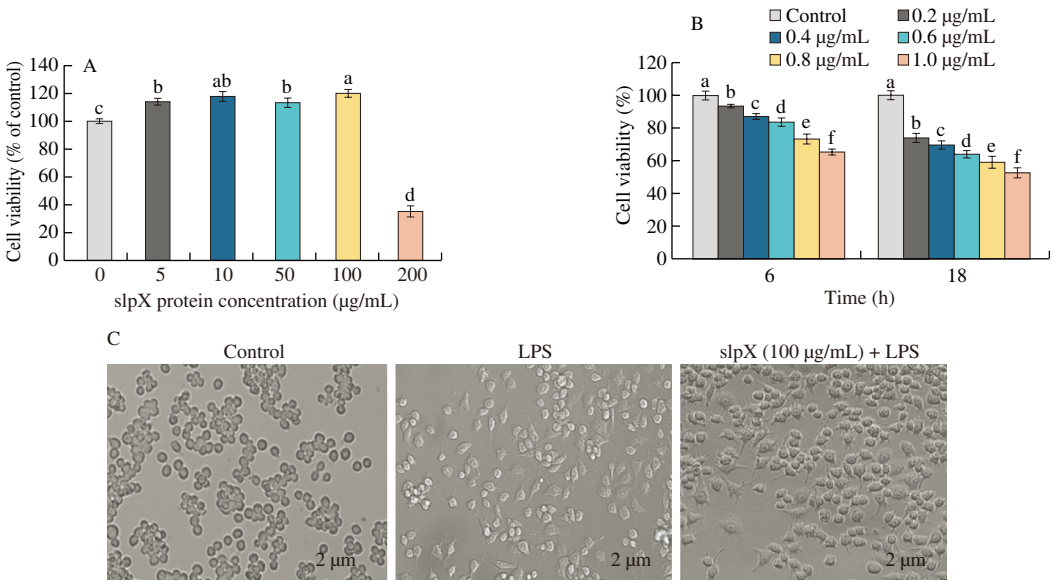

Fig. 2 Cell viability and morphological studies. (A) Cellular toxicity. Cells were treated with different concentrations of slpX for 24 h. Cytotoxicity was detected by CCK-8 assay. (B) Optimal stimulation time and concentration of LPS. Cells were stimulated with different concentrations of LPS and cell viability was detected by CCK-8 assay. (C) Changes in cell morphology observed by inverted microscope. Different lowercase letters indicate significant difference.

pathway mediates the expression of TNF-α and plays an intuitively important role in the upregulation of IL-6 and TNF-α in LPS-induced inflammation[30-31].

Similarly, Fig. 3B shows that slpX protein inhibited IL-6 more and more with increasing concentration. In particular, at the slpX protein concentration of 100 μg/mL, the secretion level of IL-6 showed a highly significant decrease compared to the LPS group, with a secretion level of only (567.1 ± 17.7) pg/mL, and the inhibition rate reached 65.09%. This may be due to the addition of slpX protein to the cells, which interacts with the TLR4/MD2 complex to form hydrogen bonds and inhibits the activation of the NF-κB signalling pathway, which is a key transcription factor driving IL-6 expression[32]. Therefore, addition of slpX protein inhibited IL-6 release induced by LPS-stimulated cells.

To learn more about understand the immunomodulatory mechanism of slpX, the secretion level of IL-10 was measured using an Elisa kit. As can be seen in Fig. 3C, the IL-10 secretion level of cells induced by LPS showed an increasing trend, which is consistent with the phenomenon described by Taverniti et al.[33] and Lund et al.[34]. Taverniti et al.[33] depicted that 1 μg/mL LPS produced 20 FOI of IL-10 compared to the blank group and that the presence of LPS increased IL-10 secretion. In the experiment, after preincubating the cells with 100 μg/mL slpX protein for 6 h, the slpX protein induced the cells to secrete a large amount of IL-10 compared to IL-10 produced by LPS, reaching 122.77 pg/mL at 6 h, which is 1.7 times the level of IL-10 secreted by LPS. This suggests that slpX proteins reduced cellular inflammation levels, and the cellular state (Fig. 2C) was improved by the intervention of slpX. Although both LPS and

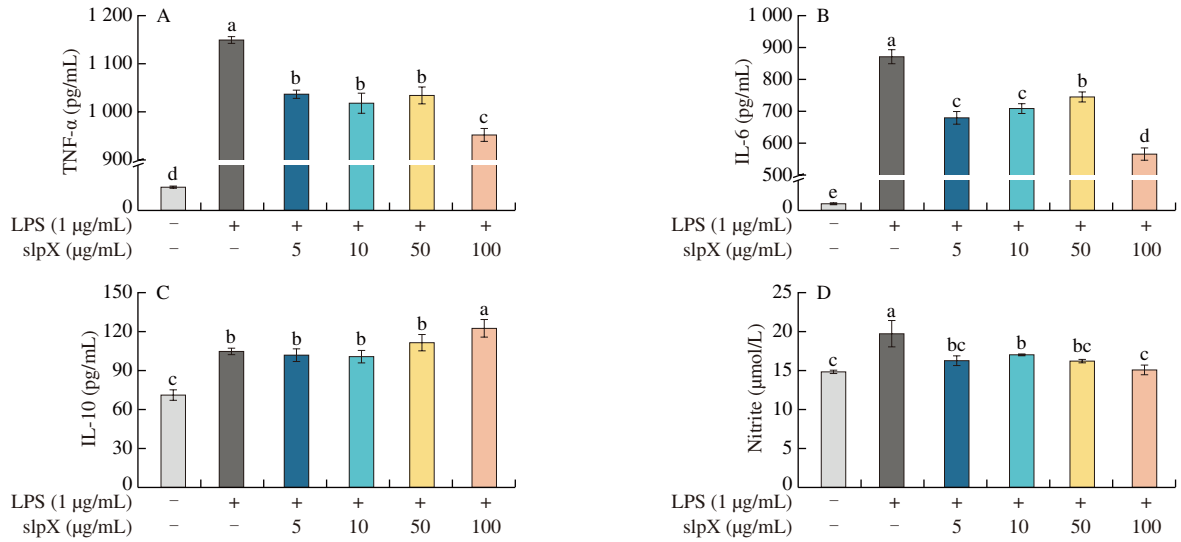

Fig. 3 In LPS-stimulated RAW264.7 cells, slpX proteins inhibit the formation of TNF-α, IL-6, and NO and promote the production of the anti-inflammatory factor IL-10. (A) TNF-α production. (B) Production of IL-16. (C) Production of IL-10. (D) NO content. Values are expressed as mean ± SD (n = 3). Different lowercase letters indicate significant differences.

slpX induced the secretion of the anti-inflammatory factor IL-10, LPS was more inclined to induce autoimmune stress when the cells were first stimulated, whereas, in contrast, slpX proteins brought more protective effects to the cells.

3.4 SlpX protein inhibits NO and ROS release in LPS-stimulated RAW264.7 macrophages

NO is a multifunctional gaseous transmitter that aids a range of physiological and pathological mechanisms at the cellular level; however, excessive NO concentrations can trigger an inflammatory response in the body[35-36]. As shown in Fig. 3D, the NO secretion level in the supernatant of control cells was low ((14.80 ± 0.20) μmol/L); pretreatment of cells with 5−100 μg/mL slpX protein significantly inhibited NO production relative to that of the LPS group ((19.74 ± 1.60) μmol/L) in a concentration-dependent manner, with 100 μmol/L of slpX bringing cellular NO secretion only reached 15.07 μmol/L. In addition, the fluorescence levels of NO and ROS in the cells were measured with DAF-FM DA and DCFH-DA (Figs. 4A and B), and it was found that the fluorescence intensities of NO and ROS in the cells were significantly increased after 18 h of stimulation with LPS alone. The fluorescence intensity of cells pretreated with 5−100 μg/mL for 6 h was significantly lower than that of the LPS-treated group. This suggests that the slpX protein, when added to RAW264.7 cells, was able to reduce cellular oxidative stress triggered by LPS stimulation, but did not lead to an optimally healthy cell. This result is consistent with the results of Wang et al.[29] who demonstrated that S-layer proteins from *L. acidophilus* NCFM reduced the level of ROS in RAW264.7 cells stimulated by LPS.

3.5 Analysis of WB

To further elucidate the mechanism by which LPS-induced activation of RAW264.7 cells regulates NO, IL-6 and TNF-α production and gene expression, the effect of slpX on the activation of the MAPK signalling pathway was determined by WB. As shown in Fig. 5A,

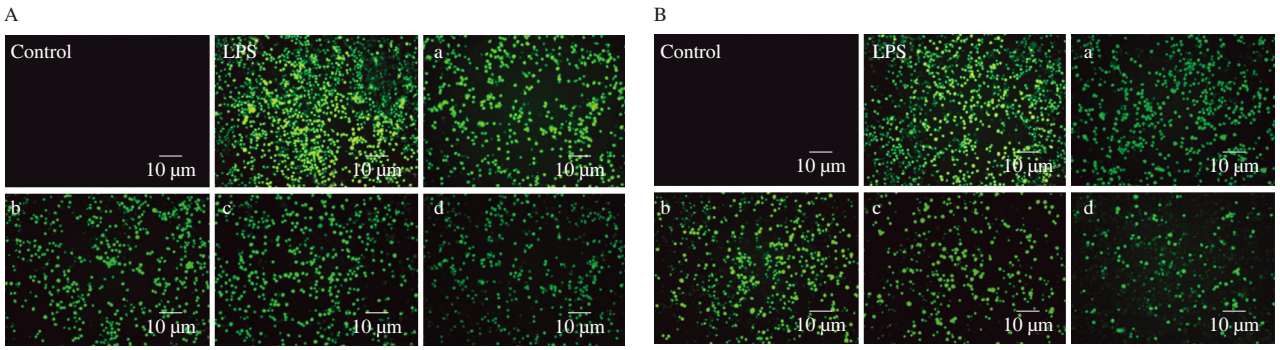

Fig. 4 slpX inhibits NO and ROS production in LPS-stimulated RAW264.7 cells. (A) Cellular fluorescence microscopy images of NO. (B) Cellular fluorescence microscopy images of ROS. The graphs a, b, c, d represents cells pretreated with different concentrations of slpX (5, 10, 50, 100 μg/mL) for 6 h and then exposed to LPS (1 μg/mL).

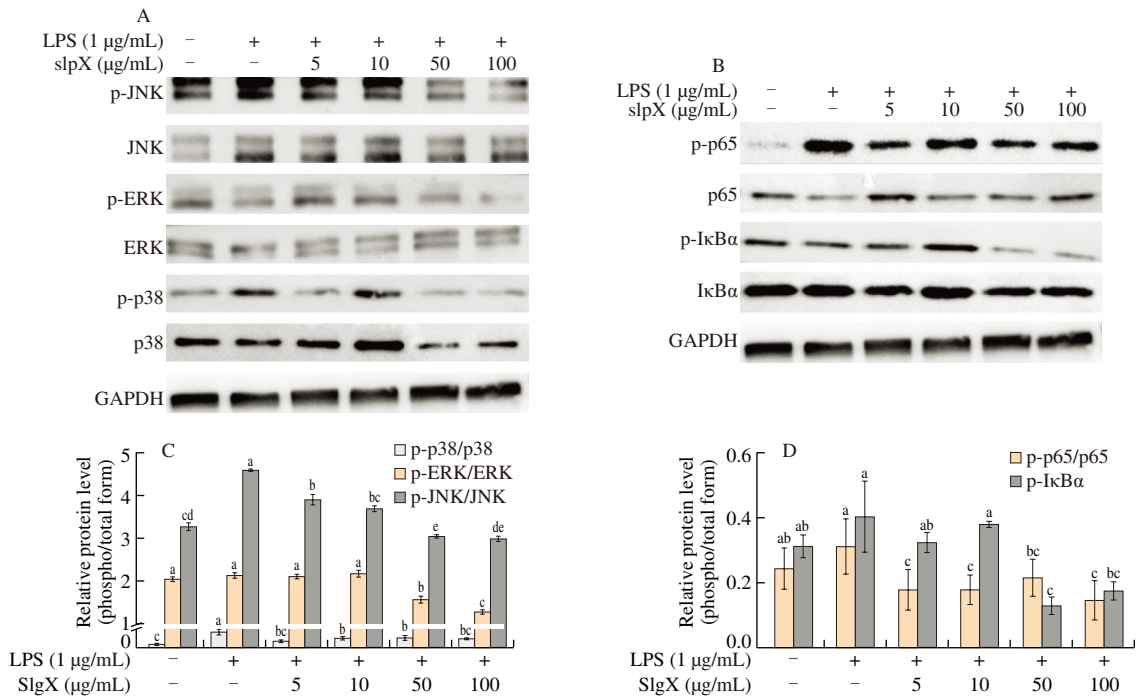

Fig. 5 slpX inhibits LPS-induced inflammatory effects in RAW264.7 cells through MAPK and NF-κB pathways. Protein expression was detected by WB. GADPH was used as a reference. Data are expressed as mean ± standard deviation (n = 3). Different lowercase letters indicate significant differences.

the phosphorylation levels of JNK, ERK, and p38 were decreased when cells were preincubated with slpX for 6 h. In particular, the expression levels of p-JNK, p-ERK and p-p38 were significantly decreased in cells pretreated with 100 μg/mL slpX. Sun et al.[37] demonstrated the anti-inflammatory effects of their substance by detecting changes in the phosphorylation levels of JNK, ERK (ERK1/2), and p38. Similarly, slpX achieved anti-inflammatory effects by decreasing the phosphorylation levels of JNK, ERK and p-38. In addition, JNK has been shown to be associated with the accumulation of NO, IL-6 and TNF-α; whereas p38 has been shown to regulate the expression of pro-inflammatory cytokines[38-40]. Wang et al.[29] showed negligible inhibition of p38 by slp, suggesting that slpX proteins have an even greater advantage in the inhibition of p38, which promotes the nuclear translocation of p65 upon phosphorylation. This implies that slpX inhibits NF-κB signalling by inhibiting the MAPK pathway.

The levels of cell viability and cytokine production indicated that slpX promoted the immunomodulatory function of RAW264.7 cells. In this study, the role of slpX in the regulation of related factors upstream of the NF-κB signalling pathway was investigated by Western blot analysis. After cells were pretreated with 100 μg/mL of slpX for 6h, the decreased levels of phosphorylation of IκBα and p65 were significantly inhibited (Fig. 5B). Meanwhile, LPS stimulation of the cells resulted in an increase in p65 expression in the nucleus, whereas slpX pretreatment of the cells resulted in a significant decrease in p65 expression in the nucleus (Fig. 6). The S-layer protein from *L. acidophilus* NCFM has been reported to inhibit the nuclear translocation of p65 and phosphorylation of IκBα to regulate the NF-κB pathway as an anti-inflammatory effect, which is similar to the effect of the slpX protein from *L. acidophilus* CICC6074 that we found, so that slpX could reduce LPS induction by inhibiting the phosphorylation of IκBα and p65 in the NF-κB signalling pathway. phosphorylation of NF-κB signalling pathways to reduce LPS-induced inflammation in RAW264.7 cells.

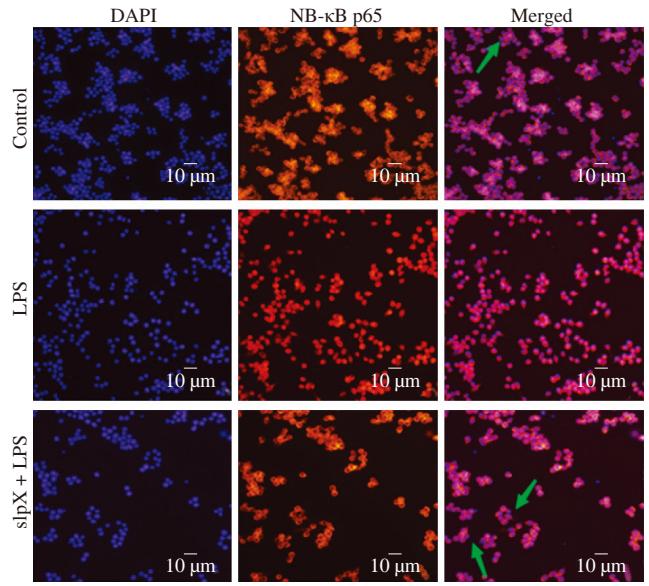

Fig. 6 slpX inhibits LPS-stimulated NF-κB p65 nuclear translocation in RAW264.7 cells. Nuclear translocation of NF-κB p65 was assessed under fluorescence microscopy. Images of the red region (representing the red region (representing the region containing p65) and the blue region (representing the DAPI-conjugated portion of the cell nucleus) are superimposed and form purple fluorescence in the confocal region.

3.6 SlpX protein downregulates LPS-stimulated RAW264.7 nuclear translocation of NF-κB in macrophages

SlpX triggers the MAPK signalling pathway by upregulating p-JNK, p-ERK and p-p38 and induces nuclear translocation of NF-κB. As shown in Fig. 6, p65 was significantly translocated to the nucleus after LPS stimulation of RAW264.7 macrophages, p65 was translocated from the nucleus to the cytoplasm when the concentration of slpX protein was 100 μg/mL. Isoquinuclidin (ISL) has been reported to inhibit inflammation induced by LPS by inhibiting the nuclear translocation of NF-κB p65[41]. This has the same result as our finding that slpX protein can inhibit pro-inflammatory mediators by inhibiting NF-κB p65 translocation to the nucleus. The results of the present study suggest that slpX proteins can suppress LPS-induced inflammation by inhibiting NF-κB p65 nuclear translocation.

3.7 Modelling the binding of slpX protein to the TLR4/MD2 complex

LPS binds to the TLR4/MD2 complex on the cell membrane and stimulates the NF-κB signalling pathway, leading to high expression of pro-inflammatory genes, including iNOS, IL-12 and TNF-α[42]. The possible binding sites of slpX proteins with human and mouse TLR4/MD2 complexes were modelled using molecular docking methods (Figs. 7A and B). The results showed (Fig. 7A) that in the two-dimensional interaction between slpX and human TLR4/MD2 complex, the negatively charged ASP122 in the slpX band chain formed a salt-bridge interaction with LYS58 of MD2 (Supplementary Material). In three-dimensional interaction results, slpX protein can form many hydrogen bonding interactions with MD2, and TLR4. In Fig. 7A, ASN235 of TLR4 formed a hydrogen bonding interaction with ASN169 of slpX with a hydrogen bonding distance of 2.7. In Fig. 7B simulation of slpX protein and TLR4/MD2 in mice, it was found that LYS152, a positively charged LYS152 of the slpX band chain, formed a salt-bridging interaction with Glu602, a negatively charged Glu602 of MD2. ASN56 of TLR4, GLU114, LYS101, LYS145, and ASP151 form hydrogen-bonding interactions with ARG256, LYS153, ASN57, GLU30, and GLN603 of the slpX protein; these interactors form a stable ternary complex.

The molecular docking results showed that slpX and TLR4/MD2 did have hydrogen-bonding interactions, which further confirmed our speculation that slpX recognised the TLR4/MD2 receptor and inhibited the degradation of protein phosphorylation on the MAPK and NF-κB signalling pathways, thereby blocking the inflammatory response induced by LPS[42].

4. Conclusion

In this study, a single highly pure protein was obtained by heterologous expression and purification of slpX protein from *L. acidophilus* CICC6074. A model of LPS-induced inflammation was developed and the protein was found to inhibit inflammation produced by LPS-stimulated RAW264.7 macrophages. Further studies showed that slpX protein effectively reduced the production of ROS, NO and inflammatory factors by inhibiting MAPK and NF-κB pathways. And whether slpX protein can trigger PKC signalling cascade to regulate the stimulatory effect of *L. acidophilus* CICC6074 will be explored

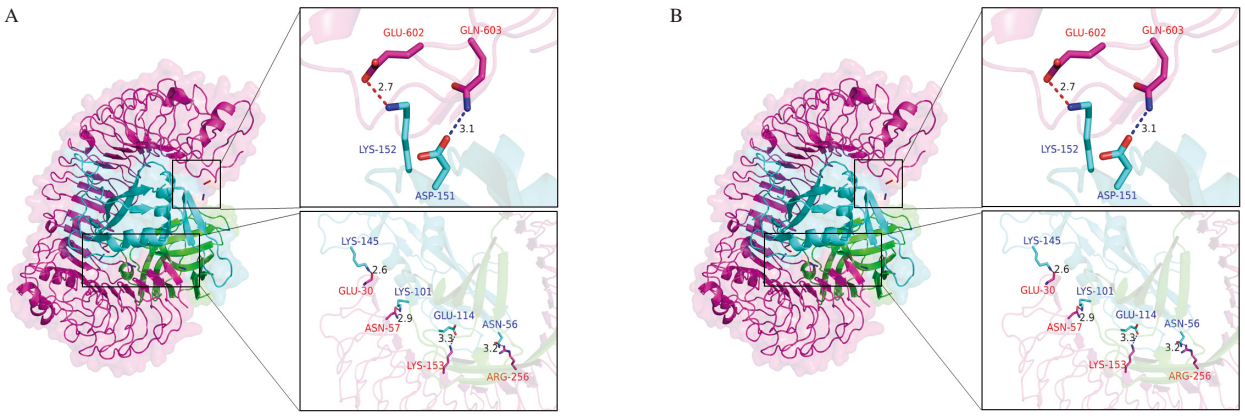

Fig. 7 The slpX protein may bind to the TLR4/MD2 complex. (A) Band model showing binding of slpX protein to human TLR4/MD2 complex (PDB: 3FX1, left), slpX (PDB: 7QF1). Squares indicate binding sites and are enlarged (right). (B) Band model showing binding of slpX protein to mouse TLR4/MD2 complex (PDB: 3VQ2, left), slpX (PDB: 7QF1). Green represents MD2, sky blue represents slpX, purple represents TRL4, green dashed lines represent hydrogen bonds, and red represents salt-bridge bonds.

in future studies in addition. The molecular docking results showed that slpX protein and TLR4/MD2 complex reduced LPS-induced cellular inflammatory responses through hydrogen bonding, and this study provides new insights into the immunomodulatory properties of *Lactobacillus* surface proteins.

Conflict of interest

The authors declare that they have no known competing financial interests or personal relationships that could have appeared to influence the work reported in this paper.

Acknowledgements

This work was supported by the National Natural Science Foundation of China (32272339), and National Key R&D Program of China (2021YFD2100104).

References

[1] R.D. Ayivi, S.A. Ibrahim, Lactic acid bacteria: an essential probiotic and starter culture for the production of yoghurt, Int. J. Food Sci. Technol. 57 (2022) 7008-7025. https://doi.org/10.1111/ijfs.16076.

[2] S.W. Cho, J. Yim, S.W. Seo, Engineering tools for the development of recombinant lactic acid bacteria, Biotechnol. J. 15 (2020) e1900344. https://doi.org/10.1002/biot.201900344.

[3] E. Ringø, S.H. Hoseinifar, K. Ghosh, et al., Lactic acid bacteria in finfish-an update, Front. Microbiol. 9 (2018) 376234. https://doi.org/10.3389/fmicb.2018.01818.

[4] T. Zhang, Y.X. Guo, X.K. Fan, et al., Protection mechanism of metal ion pre-stress on *Lactobacillus acidophilus* CICC 6074 under acid tolerance, J. Agric. Food Chem. 71 (2023) 13304-13315. https://doi.org/10.1021/acs.jafc.3c01970.

[5] D. Alp, H. Kuleaşan, Adhesion mechanisms of lactic acid bacteria: conventional and novel approaches for testing, World J. Microbiol. Biotechnol. 35 (2019). https://doi.org/10.1007/s11274-019-2730-x.

[6] M.F. Mazzeo, A. Reale, T.D. Renzo, et al., Surface layer protein pattern of *LeviLactobacillus brevis* strains investigated by proteomics, Nutrients 14 (2022) 3679. https://doi.org/10.3390/nu14183679.

[7] M. Sara, U.B. Sleytr, S-Layer proteins, J. Bacteriol. 182 (2000) 859-868. https://doi.org/10.1128/JB.182.4.859-868.2000.

[8] U. Hynönen, A. Palva, *Lactobacillus* surface layer proteins: structure, function and applications, Appl. Microbiol. Biotechnol. 97 (2013) 5225-5243. https://doi.org/10.1007/s00253-013-4962-2.

[9] S. Suzuki, K. Yokota, S. Igimi, et al., Comparative analysis of immunological properties of S-layer proteins isolated from *Lactobacillus strains*, Microbiology 165 (2019) 188-196. https://doi.org/10.1099/mic.0.000766.

[10] X. Gao, L. Huang, L.Q. Zhu, et al., Inhibition of H9N2 virus invasion into dendritic cells by the S-layer protein from *L. acidophilus* ATCC 4356, Front. Cell. Infect. Microbiol. 6 (2016) 137. https://doi.org/10.3389/fcimb.2016.00137.

[11] C.H. Xue, L.W. Zhang, H.B. Li, et al., Functionality of the S-layer proteins from *Lactobacillus* in the competitive against enteropathogens infection, Eur. Food. Res. Technol. 236 (2012) 249-255. https://doi.org/10.1007/s00217-012-1871-z.

[12] W.M. Zhang, H.F. Wang, J.X. Liu, et al., Adhesive ability means inhibition activities for *Lactobacillus* against pathogens and S-layer protein plays an important role in adhesion, Anaerobe 22 (2013) 97-103. https://doi.org/10.1016/j.anaerobe.2013.06.005.

[13] D. Li, M. Wu, Pattern recognition receptors in health and diseases, Signal Transduct. Target Ther. 6 (2021) 291. https://doi.org/10.1038/s41392-021-00687-0.

[14] A.M. Kabat, E.J. Pearce, Inflammation by way of macrophage metabolism, Science 356 (2017) 488-489. https://doi.org/10.1126/science.aan2691.

[15] C. Shi, E.G. Pamer, Monocyte recruitment during infection and inflammation, Nat. Rev. Immunol. 11 (2011) 762-774. https://doi.org/10.1038/nri3070.

[16] K. Nikovics, A.L. Favier, Macrophage identification in situ, Biomedicines 9 (2021) 1393. https://doi.org/10.3390/biomedicines9101393.

[17] P. Arulselvan, W.S. Tan, S. Gothai, et al., Anti-inflammatory potential of ethyl acetate fraction of *Moringa oleifera* in downregulating the NF-κB signaling pathway in lipopolysaccharide-stimulated macrophages, Molecules 21 (2016) 1452. https://doi.org/10.3390/molecules21111452.

[18] M. Malamud, P. Carasi, M.H. Assandri, et al., S-layer glycoprotein from *Lactobacillus kefiri* exerts its immunostimulatory activity through glycan recognition by Mincle, Front Immunol. 10 (2019) 1422. https://doi.org/10.3389/fimmu.2019.01422.

[19] F. Subhan, H.Y. Kang, Y. Lim, et al., Fish scale collagen peptides protect against $CoCl_2$/TNF-α-induced cytotoxicity and inflammation *via* inhibition of ROS, MAPK, and NF-κB pathways in HaCaT cells, Oxid. Med. Cell. Longev. 2017 (2017) 1-17. https://doi.org/10.1155/2017/9703609.

[20] A.M.G.K. Athapaththu, K.T. LEE, M.H.D. Kavinda, et al., Pinostrobin ameliorates lipopolysaccharide (LPS)-induced inflammation and endotoxemia by inhibiting LPS binding to the TLR4/MD2 complex, Biomed. Pharmacother. 156 (2022) 113874. https://doi.org/10.1016/j.biopha.2022.113874.

[21] H.J. Boot, C.P. Kolen, J.M. Noort, et al., S-layer protein of *L. acidophilus* ATCC 4356: purification, expression in *Escherichia coli*, and nucleotide sequence of the corresponding gene, J. Bacteriol. 175 (1993) 6089-6096. https://doi.org/10.1128/jb.175.19.6089-6096.1993.

[22] T. Zhang, D.D. Pan, Y.J. Yang, et al., Effect of *Lactobacillus acidophilus* CICC 6074 S-layer protein on colon cancer HT-29 cell proliferation and apoptosis, J. Agric. Food Chem. 68 (2020) 2639-2647. https://doi.org/10.1021/acs.jafc.9b06909.

[23] M. Arbabi-Ghahroudi, J. Tanha, R. MacKenzie, Prokaryotic expression of antibodies, Cancer Metast. Rev. 24 (2005) 501-519. https://doi.org/10.1007/s10555-005-6193-1.

[24] Z.W. Ji, J.Q. Mao，S.G. Chen, et al., Antioxidant and anti-inflammatory activity of peptides from foxtail millet (*Setaria italica*) prolamins in HaCaT cells and RAW264.7 murine macrophages, Food Biosci. 36 (2020) 100636. https://doi.org/10.1016/j.fbio.2020.100636.

[25] L.A. Abdulkhaleq, M.A. Assi, R. Abdullah, et al., The crucial roles of inflammatory mediators in inflammation: a review, Vet. World 11 (2018) 627-635. https://doi.org/10.14202/vetworld.2018.627-635.

[26] K. Dhaliwal, E. Scholefoeld, D. Ferenbach, et al., Monocytes control second-phase neutrophil emigration in established lipopolysaccharide-induced murine lung injury, Am. J. Respir. Crit. Care Med. 186 (2012) 514-24. https://doi.org/10.1164/rccm.201112-2132oc.

[27] S. Faller, F. Hausler, A. Goeft, et al., Hydrogen sulfide limits neutrophil transmigration, inflammation, and oxidative burst in lipopolysaccharide-induced acute lung injury, Sci. Rep. 8 (2018) 14676. https://doi.org/10.1038/s41598-018-33101-x.

[28] P.J. Murray, Macrophage polarization, Ann. Rev. Physiol. 79 (2017) 541-566. https://doi.org/10.1146/annurev-physiol-022516-034339.

[29] H.F. Wang, L. Zhang, S.C. Xu, et al., Surface-layer protein from *Lactobacillus acidophilus* NCFM inhibits lipopolysaccharide-induced inflammation through MAPK and NF-κB signaling pathways in RAW264.7 cells, J. Agric. Food Chem. 66 (2018) 7655-7662. https://doi.org/10.1021/acs.jafc.8b02012.

[30] M. Ji, Y.L. Lu, C.H. Zhao, et al., C5a Induces the synthesis of IL-6 and TNF-α in rat glomerular mesangial cells through MAPK signaling pathways, Plos One 11 (2016). https://doi.org/10.1371/journal.pone.0161867.

[31] Y.f. Shi, J.X. Chen, S.L. Li, et al., Tangeretin suppresses osteoarthritis progression *via* the Nrf2/NF-κB and MAPK/NF-κB signaling pathways, Phytomedicine 98 (2022) 153928. https://doi.org/10.1016/j.phymed.2022.153928.

[32] F.Q. Hu, D. Song, Y.M. Yan, et al., IL-6 regulates autophagy and chemotherapy resistance by promoting BECN1 phosphorylation, Nat. Commun. 12 (2021) 3651. https://doi.org/10.1038/s41467-021-23923-1.

[33] V. Taverniti, M. Stuknyte, M. Minuzzo, et al., S-layer protein mediates the stimulatory effect of *Lactobacillus helveticus* MIMLh5 on innate immunity, Appl. Environ. Microb. 79 (2013) 1221-1231. https://doi.org/10.1128/aem.03056-12.

[34] N.C. Lund, Y. Kayode，M.R. McReynolds, et al., mTOR regulation of metabolism limits LPS-induced monocyte inflammatory and procoagulant responses, Commun. Biol. 5 (2022). https://doi.org/10.1038/s42003-022-03804-z.

[35] S. Singh, Updates on versatile role of putative gasotransmitter nitric oxide: culprit in neurodegenerative disease pathology, ACS Chem. Neurosci. 11 (2020) 2407-2415. https://doi.org/10.1021/acschemneuro.0c00230.

[36] D.S. Simpson, J.Y. Pang, A. Weir, et al., Interferon-γ primes macrophages for pathogen ligand-induced killing *via* a Caspase-8 and mitochondrial cell death pathway, Immunity 55 (2022) 423-441.e9. https://doi.org/10.1016/j.immuni.2022.01.003.

[37] D. Sun, W.Y. Li, S.H. Chen, et al., shRNA-mediated suppression of γ-synuclein leading to downregulation of p38/ERK/JNK phosphorylation and cell cycle arrest in endometrial cancer cells, Mol. Biol. 54 (2020) 1006-1017. https://doi.org/10.31857/S0026898420060117.

[38] H.S. Liu, C.E. Pan, Q.G. Liu, et al., Effect of NF-κB and p38 MAPK in activated monocytes/macrophages on pro-inflammatory cytokines of rats with acute pancreatitis, World J. Gastroenterol. 9(11) (2003). https://doi.org/10.3748/wjg.v9.i11.2513.

[39] E.D. Chan, K.R. Morris, J.T. Belisle, et al., Induction of inducible nitric oxide synthase-NO by lipoarabinomannan of *Mycobacterium tuberculosis* is mediated by MEK1-ERK, MKK7-JNK, and NF-κB signaling pathways, Infect. Immun. 69 (2001) 2001-2010. https://doi.org/10.1128/iai.69.4.2001-2010.2001.

[40] J. Størling, J. Binzer, A.K. Andersson, et al., Nitric oxide contributes to cytokine-induced apoptosis in pancreatic beta cells *via* potentiation of JNK activity and inhibition of Akt, Diabetologia 48 (2005) 2039-2050. https://doi.org/10.1007/s00125-005-1912-2.

[41] M. Li, G.C. Lu, X. Ma, et al., Anti-inflammation of isoliquiritigenin *via* the inhibition of NF-κB and MAPK in LPS-stimulated MAC-T cells, BMC Vet. Res. 18 (2022). https://doi.org/10.1186/s12917-022-03414-1.

[42] A. Ciesielska, M. Matyjek, K. Kwiatkowska, TLR4 and CD14 trafficking and its influence on LPS-induced pro-inflammatory signaling, Cell. Mol. Life Sci. 78 (2020) 1233-1261. https://doi.org/10.1007/s00018-020-03656-y.